Underwater Image Dehazing Based on Disparity Estimation and Color Constraint

Yan Liu [1], Qingwu Li[2], Guanying Huo[3], Yan Zhou[4] and Dabin Yu [5]
Hohai University, Key Laboratory of Sensor Networks and Environmental Sensing, Changzhou, China
[1]E-mail: liuyan_s@163.com Tel: +86-519-85191812
[2]E-mail: li_qingwu@163.com Tel: +86-519-85191905
[3]E-mail: huoguanying@163.com Tel: +86-519-85192015
[4]E-mail: strangeryan@163.com Tel: +86-519-85288610
[5]E-mail: yudadabing@hhu.edu.cn Tel: +86-519-85288610

***Abstract*—For underwater image quality improvement, we regard image restoration as dehazing problem, and proposed a restoration method combining disparity map and color constraints. According to the dark channel prior model, image can be recovered through the estimation of background light and transmission. Considering the consistency of disparity map and depth information, the disparity map and dark channel are fused in the non-subsampled contour wave transform domain. Then the background light closer to true depth in RGB color space is estimated by the fused map with haze-lines theory. In consideration of the different attenuation characteristics of different wavelengths light in water, the transmission estimation is established according to the red-based attenuation coefficient ratio. It is benefit to improve the color distortions especially in the texture area. The experiment results show that the proposed underwater restoration image method can achieves better brightness and contrast enhancement, the image edge sharpness and color recovery.**

I. Introduction

Underwater image quality is lower than outdoor imaging because water optical properties and water medium structure are uncertain and complex. Unsatisfactory illumination intensity causes uneven illumination, and the different attenuation coefficients of various wavelength give rise to color distortion. The existence of scattering effect makes many stray lights (i.e. background light) enter the camera together with the reflected light of the target, which makes the underwater image appear atomization effect. Therefore, the image restoration process can be regarded as the dehazing process.

Dehazing algorithms based on image enhancement focus on improving image contrast, such as histogram equalization [1], Retinex algorithm [2], homomorphic filtering [3], etc.. Dehazing methods based on image restoration, such as dark channel prior (DCP) [4], focus on background light estimation and transmittance estimation. Supposing the texture and color features is prominent both in target and background region, an image distinct can be selected as the background light with gradient information, histogram statistical information, or non-local prior [5]. The global background light also can be estimated by adjustment of light source color [6], graph cut algorithm [7], or neural networks [8]. In accordance with the prior information and the different attenuation coefficient of RGB channel, transmission map can be optimized by their difference or fusion [9-11]. Furthermore, the neural network methods based on atmospheric degradation model [12] or end to end deep learning also are used to haze removal [13] [14].

These methods estimate the transmission and rely to some extent of the DCP method which was proven empirically on outdoor scenes, but their assumptions do not always hold underwater scenes. With the increase of underwater imaging distance, the absorption of light by water becomes more obvious. The different wavelengths' attenuation is dissimilar. The typical character is the faster attenuation of red light than blue and green ones. The directly using of original DCP model may cause depth of field (DOF) estimation mistake, such as color deviation (as shown in Fig. 1 (c), the fish body and sea water are blue) and non-significant dehazing effect.

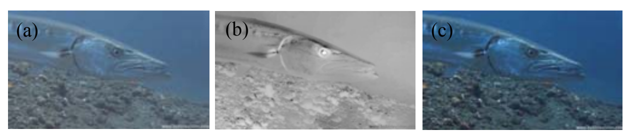

Fig. 1 Image dehazing by DCP model
(a) original; (b) transmission map; (c) restored map

When we estimate the background light attenuation coefficient and scattering coefficient, considering the different transmission characteristics of RGB channels is beneficial to ameliorate the image bias problem. In addition, the pixel value of RGB channel changes more significantly with the increasing DOF in underwater images. The intensity of corresponding dark channel increases synchronously. The depth information in disparity map obtained from binocular images directly represents the target distance and gives expression to target edge information. We can fuse disparity map and dark channel to obtain dark channel prior. That can improve block phenomenon in order to estimate precise global background light.

Therefore, we proposed an underwater image dehazing method based on disparity estimation and color constraint. In Sect. II, we present our dehazing method separately from background light and transmission estimation. In Sect. III, we show the dehazing results, and take comparison with stare-ofart methods to evaluate the performance of the proposed methods. Sect. IV concludes our work and future research challenges.

II. PROPOSED APPROACH

Based on the DCP method, we first apply disparity estimation to background light estimation calculation, and approach image restoration of various water bodies by combining with haze-lines estimation of color space. The depth information of the disparity map was fused with the dark primary color prior in the NSCT domain, and the background light in RGB space was obtained by combining the haze-lines theory. Then we develop transmission estimation model based on the attenuation coefficient of red channel. According to the Schechner model, the underwater image is restored by our recovery model with the estimated background light and transmittance. The procedure of the proposed algorithm is shown in Fig. 2.

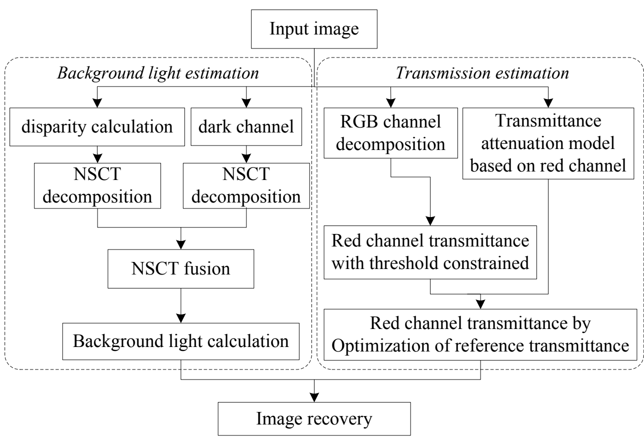

Fig. 2. Procedure of the proposed algorithm

A. Background Light Estimation Based on Disparity Estimation and Haze-lines Prior

Nonsubsampled contourlet transform (NSCT) is one of contourlet transform method [15], which takes on translational invariance. Supposing the image is decomposed to S scales with eight directions at each scale, the reference coefficient has eight neighbors in the same sub-band. The same spatial location of coarse scale is defined as father coefficient, while the sub-band of different directions in the same scale is defined as brother coefficient. To achieve fusion of disparity map and dark channel map, the correlation between neighborhood and brother coefficient is used for feature detection.

We define the fuzzy factor N_b which is determined by the low-frequency coefficient of the original dark channel. $C_{dark1}(x,y)$ and $C_{dis1}(x,y)$ are respectively low-frequency coefficients of original dark channel and disparity map, the fused image $C_1(x,y)$ can be defined as:

$$C_1(x,y)=(1-N_b)C_{dark1}(x,y)+N_bC_{dis1}(x,y) \tag{1}$$

The image's second to S scale corresponds to its high frequency coefficient. The coefficient of fused image can be calculated according to neighborhood information at each scale and brother coefficient in eight directions. At the i-direction and j-scale of high frequency sub-band, the NSCT coefficient of pixel (x,y) is defined as $C_j^i(x,y)$, and the neighborhood information at each scale is defined as regional energy :

$$E_j^i(x,y)=\sum_{(m,n)}\left(C_j^i(x+m,y+n)\right)^2,(m,n)\ is\ 3\times 3 \tag{2}$$

The brotherly correlation $\rho\left(C_j^{ip},C_j^{iq}\right)$ is used to represent the relationship between high frequency coefficients in different directions on the same scale. The brother coefficient of the subband at the same direction is normalized, and its correlation weight $W_{C_j^{ip}}$. The greater the correlation weight, the higher the brother coefficient at ip direction of j scale. The features measurement $M_j^{ip}(x,y)$ of any pixel point is defined as:

$$M_j^{ip}(x,y)=\sum_{ip,iq\in\{1,\cdots,8\},ip\neq iq}E_j^{ip}(x,y)W_{C_j^{ip}}\left(C_j^{ip}\right) \tag{3}$$

For the fusion between two images, the high frequency coefficient with a larger characteristic measurement value will be chosen to be the high frequency coefficient after fusion as follows:

$$C_j^i(x,y)=\begin{cases}C_{darkj}^i(x,y), if\ M_{darkj}^i(x,y)\geq M_{disj}^i(x,y)\\ C_{disj}^i(x,y), else\end{cases} \tag{4}$$

According to the image haze removal theory in references [16] and [27], as far as a haze-free image, pixel value distribution in each color space is a class of RGB space; as far as a haze image, the corresponding distribution is a line which is called haze-lines [18]. Due to the different foggy levels in different regions, there may be several haze-lines in one image, and multiple regions may belong to the same haze-line. The haze-line $H(x)$ is represented as:

$$H(x)=\left(1-I_R(x)\right)-\max(I_B(x),I_G(x)) \tag{5}$$

If the target is at infinite point, the red channel attenuation was close to 0. At this moment, the pixel value is the haze-line value. We arrange the pixel values in fused dark channel map from smallest to largest, and take on the top 10% pixels (usually are the larger depth of field). Then the pixels with lower pixel values in each color space are searched in the corresponding positions of original image. The value of these pixels are the background light A_R, A_G and A_B.

B. Transmission Estimation Based on Red Channel Reference Attenuation Ratio

The environment is dissimilar in various water types because of the dissolved substances, suspended matter, sediment, aquatic organisms, etc.. Thus, there are different of light absorption and scattering coefficients. Ref. [19] gives the approximate attenuation coefficients of different sea areas and coastal waters. We utilize these coefficients to estimate transmittance for RGB channel.

The farther the underwater optical imaging distance is, the more light is absorbed by the water body. $\beta_\lambda\left(\lambda=R,G,B\right)$ is the attenuation coefficient of water body in different channel. The water transmittance is related to the light propagation distance as shown as:

$$t_\lambda(x)=e^{-\beta_\lambda d(x)} \tag{6}$$

Substituting (6) into Schechner model with considering RGB color space, there is

$$\begin{cases} A_R-I_R=e^{-\beta_R d(x)}(A_R-J_R) \\ A_G-I_G=e^{-\beta_G d(x)}(A_G-J_G) \\ A_B-I_B=e^{-\beta_B d(x)}(A_B-J_B) \end{cases} \tag{7}$$

In order to reduce the transmittance calculation error caused by attenuation coefficient error, the attenuation ratio can be introduced. The attenuation coefficient ratio is respectively defined as $\beta_{RG}=\beta_R/\beta_G$ and $\beta_{RB}=\beta_R/\beta_B$.

$$\begin{cases} (A_G-I_G)^{\frac{\beta_R}{\beta_G}}=e^{-\beta_G d(x)\cdot\frac{\beta_R}{\beta_G}}(A_G-J_G)^{\frac{\beta_R}{\beta_G}} \\ (A_B-I_B)^{\frac{\beta_R}{\beta_B}}=e^{-\beta_B d(x)\cdot\frac{\beta_R}{\beta_B}}(A_B-J_B)^{\frac{\beta_R}{\beta_B}} \end{cases} \tag{8}$$

Color number is much less than pixel number in one image. In Ref. [18], each channel' pixels are clustered into some fuzzy sets by k-means algorithm, then each pixel value is replaced by the center of each set. If at least one pixel in each set is a haze-free pixel, the original transmittance of RGB space can be obtained respectively. In underwater images, the attenuation coefficients of RGB space are not consistent, thus there may be non-fuzzy pixels in each fuzzy set. Taking the red channel as the benchmark, and considering the attenuation coefficient for each channel, the lower transmittance threshold t_{Rm} is defined as:

$$t_{Rm}=\max\left\{1-\frac{1-I_R}{1-A_R},(1-\frac{I_G}{A_G})^{\beta_{RG}},(1-\frac{I_B}{A_B})^{\beta_{RB}}\right\} \tag{9}$$

As we know, the attenuation of red channel is faster with long transmission distance. According to the attenuation coefficient measured by Jerlov, the attenuation coefficient of R channel is close to 0.9 when the distance is 1 meter between target and camera. The attenuation constraint threshold is defined as $1-t_R(x)$, and the red channel transmittance $t_R^0(x)$ can be obtained by:

$$t_R^0(x)=\max\left\{1-t_R(x),t_{Rm}\right\} \tag{10}$$

In the haze-lines model, the fuzzy line clustering is carried on global pixels. If there are fewer pixels in a certain set and the noise problem is serious, the restoration result for these pixels will be limited. Therefore, we introduce a smoothing term to construct the minimization function:

$$\arg\min\left\{\sum_x\frac{\left[\hat{t}_R(x)-t_R^0(x)\right]^2}{\sigma^2(x)}+\delta\sum_x\sum_{y\in N_x}\frac{\left[\hat{t}_R(x)-\hat{t}_R(y)\right]^2}{\left\|I(x)-I(y)\right\|}\right\} \tag{11}$$

where δ is the balance coefficient between data and smooth term; N_x is the neighborhood pixel of x; $\sigma(x)$ is the standard deviation obtained from haze-lines.

With the estimation for background light A_λ and transmittance map $\hat{t}_R(x)$, the underwater images can be recovered as follows:

$$J_\lambda=\frac{I_\lambda-A_\lambda}{\hat{t}_\lambda}+A_\lambda,\ \text{where } \hat{t}_G=\hat{t}_R^{\,\beta_G/\beta_R},\hat{t}_B=\hat{t}_R^{\,\beta_B/\beta_R} \tag{12}$$

III. EXPERIMENTAL RESULTS AND DISCUSSION

A. Experimental Set-up and Method

We carry out the experiment both in seawater and fresh water. And we take both qualitatively and quantitative comparisons with state-of-the-art methods.

The author of Ref. [20] provides original binocular images dataset and disparity map by EpicFlow [21]. EpicFlow is suitable for dense matching with further areas, and the low signal-to-noise-ratio images. Therefore, we directly use them for seawater experiment.

For fresh water experiment, the images were taken using a pair of IP cameras (1280H×960V resolution with focal length 5mm). The water depth was 0.6 meters, turbidity was 1.68 NTU, and the target distance was less than 1.5 meters. The disparity maps of fresh water are obtained by WCPSP [22] which is suitable for finding smoothness target edge especially at the low texture images.

The proposed method improves image quality based on dehazing model, and we make comparation with classical DCP [4], DCP based on red-channel (RDCP) [23], non-local and depth-based DCP (UDCP) [24], non-local image dehazing (NLD) [18], and underwater single image color restoration using haze-lines (UWHL) [20].

B. Recovery Results and Qualitative Comparison

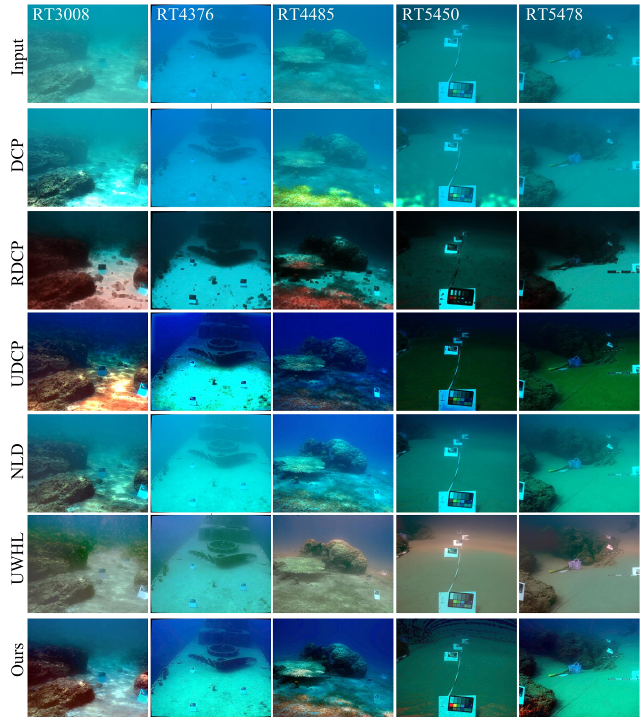

Fig. 3 Comparison of restoration results in seawater

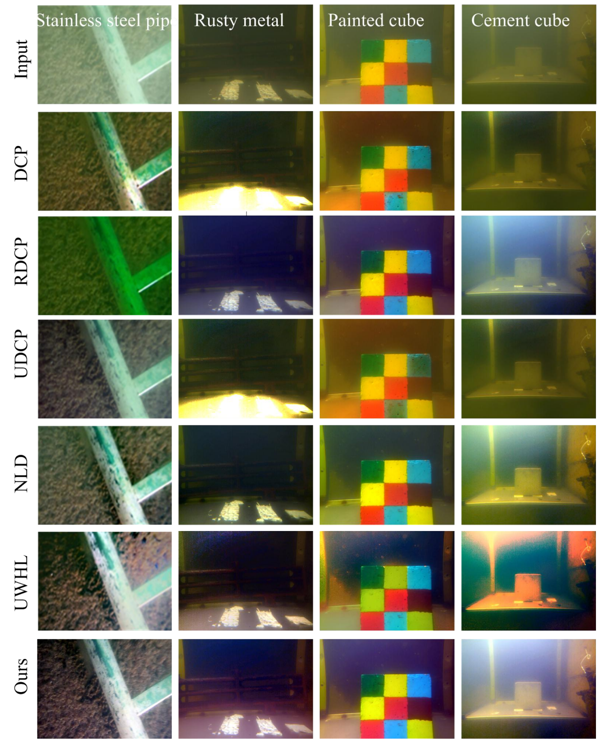

Fig. 4 Comparison of restoration results in freshwater

Fig. 3 and Fig. 4 shows the input images on the top row, followed by the output of different underwater image dehazing methods.

The DCP method estimates the global background light as a constant without considering different depth of field. As Fig. 3 shows the effect of DCP method dehazing is not observable. The RDCP and UDCP method is more effective in removing atomizing effects than the DCP method. Due to the RDCP method considering the red channel decays faster than blue and green channels, dehazing images appear to be red especially near camera region (see the results of RT3008, RT4485). The UDCP method only consider the light attenuation of blue-green channels, so the whole image appears blue or green. The NLD, UWHL and our method detect the haze-lines in different color spaces, and estimate more accurate background light for underwater images. Their effect is better especially in target location. The proposed method is more obvious comparing with NLD, and the color restoration is more natural than UWHL.

Unfortunately, there is image distortion in father region (see the results of RT5450). The mistake is caused by using disparity information for the background light estimation. The accurate calculation of disparity is difficult in low-texture domain.

As Fig. 4 shows, the image of stainless steel pipe had a slight camera shake, which resulted in a distinct blur. The RDCP method leads the whole image to be green. Although the other comparison methods perform better in fog removal, the pipe edge is not clear. The results of DCP and UWHL methods appear reflective phenomenon. At the image of rusty metal, some white attachments lead the dark channel and transmittance calculating mistakes near the camera area by the DCP and UDCP methods. The experiment of painted cube can test the effect of restoration method on color restoration. The DCP, UDCP, NLD and UWHL method have color bias, which are reddish, reddish, green and green, respectively. Because the target is relatively close, using the red channel's fast attenuation feature for transmittance estimate can obtain better color restoration effect. The results of cement cube image show that the brightness recovery is not good by DCP and UDCP methods, and the color recovery is not good by NLD and UWHL methods. The dehazing effect by the RDCP and the proposed methods is not obvious, but the edges and details of the wall attachment in the right area are clearly visible.

Due to the water turbidity and the target low-texture, the depth estimation is not accurate enough, which affects the calculation of transmittance and the final restoration result.

C. *Quantitative Evaluation*

We employ the non-reference image quality evaluation indexes to take quantitative evaluation, including mean gradient, contrast, image information entropy, underwater image sharpness measure. We calculate the four non-reference image quality evaluation indexes and separately show them in Fig. 5. The abscissa is the experiment image, and the ordinate is the index value. The larger the corresponding index value, the better the image quality. The proposed method achieves the best results almost all seawater or fresh water images. It has a good effect on target edge restoration in the image because the disparity map is used for

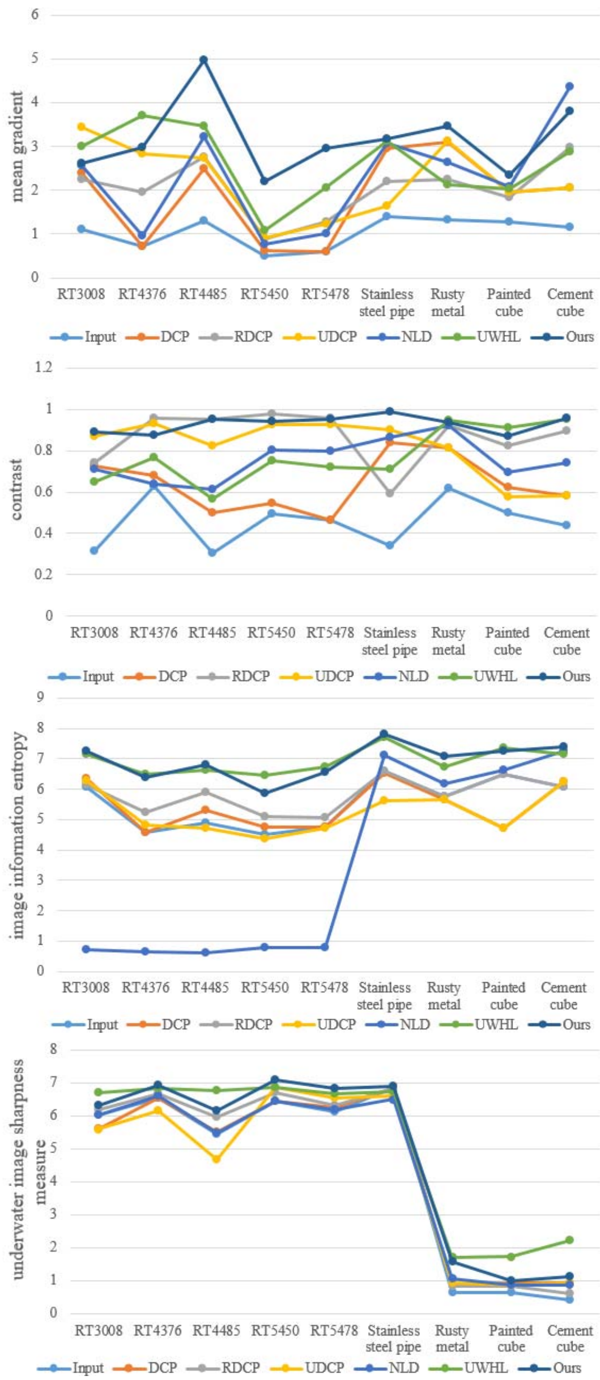

Fig. 5 Quality evaluation of each algorithm for each image

background light estimation. Although the RDCP method acquires the best contrast in the restoration of RT4376, RT 5450 and RT 5478, the target regions in the three images have poor visibility. Meanwhile, our method can retain rich information and improve the image clarity. The UWHL method obtains the highest at other images, whereas there is color deviation problem at RT4376, RT5450, RT5478, painted cube and mud cube.

Therefore, it is effective to introduced disparity information for the background estimation. Using red benchmark channel for attenuation ratios is conducive to improve transmission estimation. However, our method depends on the disparity calculation accuracy. If the water turbidity is too high, it is hard to get precise matching result at target edge. The restoration effect of the method will be compromised.

IV. CONCLUSIONS AND FUTURE WORK

We expanded the DCP model to handle underwater wavelength attenuation and background depth. Specifically, we evaluate background light by considering the binocular stereo depth information. We coalesce different frequency domain of disparity map and dark channel in NSCT domain, and pick out the best background light region. By considering the quicker attenuation of red channel, we establish the attenuation coefficient model to obtain transmittance map.

Unlike atmospheric images, underwater scenes are more complex under the water types and turbidity. The restoration experiments were carried out on the seawater and fresh images. The proposed method has better results in terms of image brightness, color fidelity and image details. However, it cannot reach the best value for all quality evaluation indexes. The disparity calculation and its integration method should be improved in subsequent work.

ACKNOWLEDGMENT

This work is supported by the Fundamental Research Funds for the Central Universities under grants B210202086.

REFERENCES

[1] X. Ding, Y. Wang, J. Zhang and X. Fu. "Underwater image dehaze using scene depth estimation with adaptive color correction." *OCEANS 2017, Aberdeen*:2017,8084665.

[2] P. Zhuang and X. Ding. "Underwater image enhancement using an edge-preserving filtering Retinex algorithm." *Multimedia Tools and Applications*, vol.79, no. 15, pp. 17257–17277, July 2020.

[3] A. Ghani and N. Isa. "Homomorphic filtering with image fusion for enhancement of details and homogeneous contrast of underwater image." *Indian Journal of Geo-Marine Sciences,* Vol. 44, pp. 1904-1919, January 2016.

[4] K. He, J. Sun, and X. Tang. "Single image haze removal using dark channel prior". *IEEE Transactions on Pattern Analysis and Machine Intelligence*. Vol. 33, no. 12, pp. 1956-1963, January 2011.

[5] D. Berman, T. Treibitz, and S. Avidan, "Single Image Dehazing Using Haze-Lines," in *IEEE Transactions on Pattern Analysis and Machine Intelligence*, vol. 42, no. 3, pp. 720-734, March 2020.

[6] M. Zhang and J. Peng, "Underwater Image Restoration Based on A New Underwater Image Formation Model," in *IEEE Access*, vol. 6, pp. 58634-58644, 2018.

[7] L. Liu, H. Bian, S. I. Yagi, and X. Yang. "A prior-knowledge-based threshold segmentation method of forward-looking sonar images for underwater linear object detection."

Japanese Journal of Applied Physics, 55(7S1):07KG06, July 2016.

[8] S. Yin, J. Xin, Y. Wang, and A. Basu. "Image dehazing with uneven illumination prior by dense residual channel attention network." *IET Image Processing*, vol. 14, no. 12, August 2020.

[9] Y. Zhou, Q. Wu, K. Yan, L. Feng, and W. Xiang, "Underwater Image Restoration Using Color-Line Model," in *IEEE Transactions on Circuits and Systems for Video Technology*, vol. 29, no. 3, pp. 907-911, March 2019.

[10] L. Zhang, S. Wang, and X. Wang. "Single image dehazing based on bright channel prior model and saliency analysis strategy." *IET Image Processing*, vol. 15, no. 5, December 2020.

[11] P. Soma and R. K. Jatoth. "An efficient and contrast-enhanced video de-hazing based on transmission estimation using HSL color model." *The Visual Computer*, April 2021.

[12] H. Sun, M. H. Ang, and D. Rus, "A Convolutional Network for Joint Deraining and Dehazing from A Single Image for Autonomous Driving in Rain," *2019 IEEE/RSJ International Conference on Intelligent Robots and Systems (IROS)*, 2019, pp. 962-969.

[13] B. Cai, X. Xu, K. Jia, C. Qing, and D. Tao, "DehazeNet: An End-to-End System for Single Image Haze Removal," in *IEEE Transactions on Image Processing*, vol. 25, no. 11, pp. 5187-5198, November 2016.

[14] A. Fahim and H. Y. Jung . "Single Image Dehazing Using End-to-End Deep-Dehaze Network." *Electronics* ,vol. 10, no. 7, pp.817, March 2021.

[15] C. Da, L. Arthur, J. P. Zhou, and M. N. Do, "The Nonsubsampled Contourlet Transform: Theory, Design, and Applications," in *IEEE Transactions on Image Processing*, vol. 15, no. 10, pp. 3089-3101, October 2006.

[16] Y. Peng and P. C. Cosman, "Underwater Image Restoration Based on Image Blurriness and Light Absorption," in *IEEE Transactions on Image Processing*, vol. 26, no. 4, pp. 1579-1594, April 2017.

[17] R. W. Gould, R. A. Arnone, and P. M. Martinolich. Spectral dependence of the scattering coefficient in case 1 and case 2 waters. Applied Optics, Vol. 38, no. 12, pp. 2377-2383,1999.

[18] D. Berman, T. Treibitz and S. Avidan, "Non-local Image Dehazing," *2016 IEEE Conference on Computer Vision and Pattern Recognition (CVPR)*, 2016, pp. 1674-1682.

[19] N. G. Jerlov. "Marine Optics." January 1976.

[20] D. Berman, D. Levy, S. Avidan, and T. Treibitz. "Underwater Single Image Color Restoration Using Haze-Lines and a New Quantitative Dataset." *IEEE Transactions on Pattern Analysis and Machine Intelligence*, March 2020.

[21] J. Revaud, P. Weinzaepfel, Z. Harchaoui, and C. Schmid, "EpicFlow: Edge-preserving interpolation of correspondences for optical flow," *2015 IEEE Conference on Computer Vision and Pattern Recognition (CVPR)*, 2015, pp. 1164-1172.

[22] Q. Yang, "Local Smoothness Enforced Cost Volume Regularization for Fast Stereo Correspondence," in *IEEE Signal Processing Letters*, vol. 22, no. 9, pp. 1429-1433, September 2015.

[23] A. Galdran, D. Pardo, A. Picón, and A. Alvarez-Gila. "Automatic Red-Channel underwater image restoration." *Journal of visual communication & image representation,* Vol. 26, no. 1, pp. 132-145, January 2015.

[24] S. Emberton, L. Chittka, and A. Cavallaro. "Hierarchical rank-based veiling light estimation for underwater dehazing." *British Machine Vision Conference,* Swansea:2015.